Thi_Qar University Journal for Engineering Sciences, Vol. 3, No. 2 2012

Study of Turbulent Flow and Heat Transfer Over a Backward-Facing Step Under Impingement Cooling

Khudheyer S. Mushatet

College of Engineering, Thiqar University

Nassiriya, Iraq

Salimhamed2000@yahoo.com

Abstract

Computations are presented to study the turbulent flow and heat transfer over a channel backward-facing step under impingement cooling. The problem was simulated for different parameters, such as the number of impinging jets, contraction ratio, size of jets, and jet and channel Reynolds numbers. The contraction ratio had the values 0.25, 0.35 and 0.5. The impinging jets were normal to the cross-channel flow. A control volume approach using staggered grid techniques was considered to integrate the continuity, fully elliptic Navier-Stockes and energy equations. A computer program was developed, and the SIMPLE algorithm was employed to determine the existence of coupling between the continuity and Navier-Stockes equations. The effect of turbulence was modelled using a k-ε model while the wall functions laws were used to treat the regions near the solid walls. The presented results show that the strength and size of recirculation regions near the reattachment region just after the backward-facing step increase as the contraction ratio increases. Also, the results show that the size of jets, number of jets, and jet and channel Reynolds numbers have a significant effect on the flow field, turbulent kinetic energy and variation of the Nusselt number.

Keywords: Impingement Cooling, Backward-Facing, Turbulent Flow.

دراسه الجريان الاضطرابي وانتقال الحرارة فوق عتبه داخل مجرى هوائي بوجود تبريد تصادمي

المستخلص

في هذا البحث تم أجراء دراسة حسابية لدراسة خصائص الجريان الأضطرابي وانتقال الحرارة فوق عتبه داخل مجرى هوائي و بوجود التبريد التصادمي. تم نمذجة المسألة المدروسة بتأثير عدة عوامل مثل حجم وعدد المنافث،نسبة التحضر وأرقام رينولدز للمجرى الرئيسي والمنافث.نسب التخصر المدروسة كان لها قيم 0.25, 0.5،0.3 على التوالي والنفاثات التصادمية كانت عمودية على المجرى الرئيسي. أستخدمت طريقة الحجم المحدد مع تقنية الشبكة الزاحفة لتكامل

معادلات الأستمرارية و ناقير-ستوكس والطاقة بينما طور برنامج حاسوب بلغة فورتران وبأعتماد خوارزمية الأجراء المبسط التي تحدد الأرتباط بين الأستمرارية ومعادلات نافير-ستوكس. أستخدم نموذج الأضطراب k-ε لنمذجة تأثير الأضطراب في الجريان. أوضحت النتائج التي تم الحصول عليها أن قوة وحجم مناطق إعادة التدوير وطول اعادة الأتصال خلف العتبة يزداد مع زيادة نسبة التخصر. أيضا بينت النتائج أن حجم وعدد المنافث وأرقام رينولدز للمجرى الرئيسي والمنافث لها تأثير واضح على مجال الجريان والطاقة الحركية للضطراب وعدد نسلت.

1. Introduction

Flow separation and reattachment phenomena occur in many engineering and technological applications, such as cooling of turbine blades, cooling of electronic devices, combustion chambers, and flows around buildings, hills and aircrafts. In some applications, the separated and re-attachment regions must be controlled to optimally enhance the heat transfer rate. In the conventional problem of a backward-facing step, however, the geometry is simple, but the resulting structure of the flow field is complicated, especially after the step where a mixing region is created. The impingement cooling mechanism are considered when fast and effective heat transfer dissipation from the hot surface is needed. This mechanism is enhanced when array of multiple impinging jets are used instead of a single jet where mixing zones between these jets are created. Thus this paper tries to conduct a study emphasis on enhancing the rate of heat transfer via incorporating array of impinging slot jets in to the problem of a backward facing step. A channel with a backward-facing step has been investigated experimentally and numerically. Lio an Hwang [1] performed a numerical study on turbulent flow in a duct with a backward-facing step. The turbulent flow and heat transfer in a channel with rib turbulators was investigated by Lio and chen [2], Rau et al. [3] and Hane and Park [4].The main objective of these studies was to obtain the heat transfer characteristics and friction factor.

Kasagi and Matsunaga [5] studied the turbulent flow in a channel with a backward facing step. 3-D particle tracking velocimeter was used as a measurement technique. They found that the Reynolds normal and shear stresses had the maximum values upstream of the re-attachment. Their study was compared with numerical simulation. Jovice and Driver [6] presented an experimental study on the turbulent flow over a backward facing step at low Reynolds number. The aim was to validate the numerical simulation which was performed by Stanford/NASA center for turbulence research. They demonstrated that the backward facing step flows were sensitive to step height and Reynolds number. ABE and Kondah[7] presented a new turbulent model for predicting fluid flow and heat transfer in separating and reattaching flows. The presented model was modified from low-Reynolds number k-ε model. They

demonstrated that the used model was efficient in separating and reattaching flows downstream of backward facing step. Ichimiya and Hosaka [8] presented an experimental study to investigate the characteristics of impingement heat transfer caused by three impinging jets. They conducted that there was two peaks of the local Nusselt number behind the second nozzle. Zhang et al. [9] developed a stochastic separation flow model to simulate the sudden expansion of particle-laden flows. A large eddy method and Lagrangian techniques were used by Wang et al. [10] to simulate the turbulent flow over a backward-facing step. The study verified that the particles follow a path when the vorticity of the gas phase is small. Thangam and Knight [11] and Nie and Armaly [12] studied the effect of step height on the separation flow for convective flow adjacent to a backward-facing step. Rhee and Sung [13] adopted a diffusive tensor heat transfer model instead of the familiar constant Prandtl number model. An experimental study was presented by Feng et al. [14] to visualise the turbulent separated flow and measure the wall pressure over a backward-facing step. The study showed that below the separation bubble and the reattachment zone, the negative peak of the time varying wall pressure was in phase with the passage of the local large scale vertical structure. Several studies have reviewed the subject of impingement cooling. Law and Masliyah [15], Chou and Hung [16] and Lee et al. [17] performed a numerical investigation on low Reynolds number impinging jets, which were used to avoid hydrodynamic pressure caused by impingement on the surface. Benna et al. [18], Park and Sung [19]and Cooper et al. [20] presented numerical studies on high Reynolds number impinging jets with different turbulence models. Beitelmal et al. [21] investigated the heat transfer distribution in the impingement region. The considered impinging jets were inclined at different angles of attack. Yang and Shyu [22] and Gabry et al. [23] used CFD models to predict the heat transfer distribution on a smooth surface under an array of angled impinging jets with cross flow. Different angles of attack and conjugate conduction in the boundary were included. The study verified that the Yang-Shih model performed better than the k-ϵ model. Four turbulence models were used by Craft et al. [24] to simulate the turbulent flow of impinging jets discharging from a circular pipe.

In this work, an attempt is made to incorporate the effect of impinging slot jets to the problem of channel backward-facing step flow. To the knowledge of the author, there is no study documented on this particular flow geometry up to date, Consequently this study will assist to promote the research area and giving new aspects to enhance the rate of heat transfer. Thus, a computational study to simulate the turbulent flow and heat transfer of multiple impinging slot jets over a backward-facing step in cross channel flow was carried out as

shown in Figure (1). The scenario was tested with different parameters, such as the contraction ratio (SR), the size and number of impinging jets, and jet and channel Reynolds numbers. The aim of the present work is to show how array of multiple confined impinging slot jets can be a controlling factor to enhance the rate of heat transfer from the hot surface of the channel backward facing step.

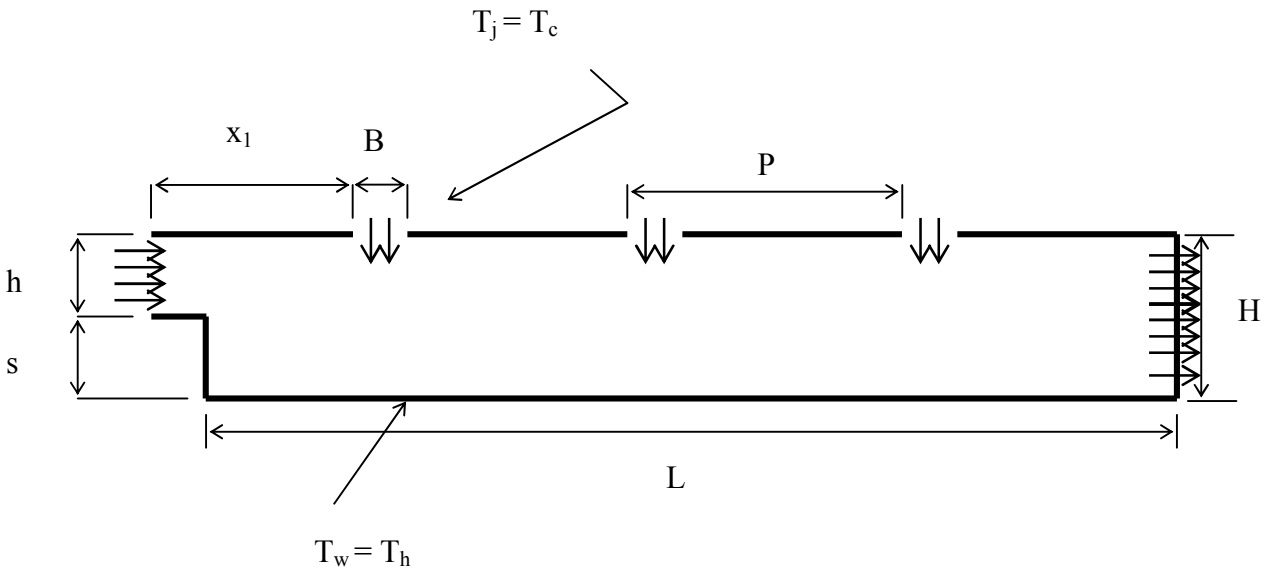

Figure (1). Schematic diagram of the considered problem, H=0.05m, L=0.4m,x_1=0.0492m, H/B=11, P/B=4 .

2. Mathematical model and numerical solution

The following assumptions are used to simplify the solution of mathematical model.

1. Steady state
2. Incompressible flow
3. Constant thermo physical properties.
4. Non slip flow
5. Steady state

The continuity, turbulent fully elliptic Navier-Stockes and energy equations are used to model the considered problem.

$$\frac{\partial}{\partial x_i}\left(\rho U_i\right) = 0 \qquad (1)$$

$$\frac{\partial U_i U_j}{\partial x_j} = \frac{-\partial P}{\partial x_i} + \frac{\partial}{\partial x_j}\left(\mu \frac{\partial U_i}{\partial x_j} - \overline{\rho u_i u_j}\right) \quad (2)$$

$$\frac{\partial U_i T_j}{\partial x_j} = \frac{\partial}{\partial x_j}\left(\frac{\mu}{\Pr}\frac{\partial T_i}{\partial x_j} - \overline{\rho u_i t_j}\right) \quad (3)$$

The turbulent stresses $\overline{\rho u_i u_j}$ and turbulent heat fluxes $\overline{\rho u_i t_j}$ should be modelled in order to close the mentioned governing equations. One of the most widely used turbulence models is the standard k-ϵ model because it has the ability to handle complex high Reynolds number flows in much less time than other complicated models. However this model gives un prediction of the flow characteristics especially in re-circulating regions as in the region downstream of backward facing, Abet and Kondoh[25].The next section in the discussion of results will offer the percentage of this un prediction for the flow and thermal field. This model solves two transport equations: one for the turbulent kinetic energy and the other for the dissipation rate of the turbulent kinetic energy, Jones and Lunder [26], as shown below:

$$\frac{\partial \rho k U_i}{\partial x_j} = \frac{\partial}{\partial x_j}\left[\left(\mu + \frac{\mu_t}{\sigma_k}\right)\frac{\partial k}{\partial x_j}\right] + \rho(G_b - \varepsilon) \quad (4)$$

$$\frac{\partial \rho \varepsilon U_j}{\partial x_j} = \frac{\partial}{\partial x_j}\left[\left(\mu + \frac{\mu_t}{\sigma_\varepsilon}\right)\frac{\partial \varepsilon}{\partial x_j}\right] + \rho\frac{\varepsilon}{k}\left(C_{1\varepsilon} G_b - C_{2\varepsilon}\varepsilon\right) \quad (5)$$

where the shear production term, (G_b), is defined as:

$$G_b = \mu_t\left(\frac{\partial u_i}{\partial x_j} + \frac{\partial u_j}{\partial x_i}\right)\frac{\partial u_i}{\partial x_j} \quad (6)$$

The turbulent viscosity is given by:

$$\mu_t = \rho C_\mu \frac{k^2}{\varepsilon} \quad (7)$$

The model coefficients are (σ_k; σ_ϵ; $C_{1\epsilon}$; $C_{2\epsilon}$; $C\mu$) = (1.0, 1.3, 1.44, 1.92, 0.09), respectively.

Boundary Conditions

At the walls: U = V = 0, k = 0, and $\frac{\partial \varepsilon}{\partial y} = 0$

At the lower wall: θ=1

At the upper wall: $\frac{\partial \theta}{\partial y} = 0$

At inlet:

$k_{in} = 0.05U_{in}^{2}$, $k_j = 0.05U_j^{2}$, $T_{in} = T_c$, $T_j = T_c$, $T_w = T_h$

$\varepsilon_{in} = k_{in}^{1.5} / \lambda H$, $\varepsilon_j = k_j^{1.5} / \lambda B$, $\lambda = 0.005$

$\mathrm{Re}_{in} = \frac{U_{in} h}{\nu}$, $\mathrm{Re}_j = \frac{U_j B}{\nu}$

where k_{in}, k_j, U_{in}, U_j, T_{in}, T_j are the turbulent kinetic energies, velocities and temperatures at a channel inlet and slot jet inlet, respectively.

The local Nu along the bottom hot wall is expressed as $Nu = \frac{\partial \theta}{\partial Y}$ at y=0.

At the channel exit, zero gradients are imposed for the dependent variables. To remedy the large steep gradients near the walls of the channel and the step, wall function laws proposed by Versteege [27] are incorporated. because they are popular and save computational resources. In this study, the numerical computations are performed on a non-uniform staggered grid system. A finite volume method (FVM) described by Versteege [27] is adopted to integrate the governing equations from (1) to (5).

$$\int_{cv} (\rho \phi u) dv = \int_{cv} div(\Gamma grad\phi) dv + \int_{cv} S_\phi dv \qquad (8)$$

Thus, a system of discretisation equations is developed, which means that the system of elliptic partial differential equations is transformed into a system of algebraic equations. Then, the solution of these transformed equations is performed by an implicit line by line Gaussian elimination scheme. An elliptic finite volume computer code was developed to attain the results of the numerical procedure by using pressure-velocity coupling (SIMPLE algorithm), according to Versteege [27]. This code is based on a hybrid scheme. Because of the strong coupling and non-linearity that are inherent in these equations, relaxation factors are needed to ensure convergence. The relaxation factors used for velocity components and the pressure, temperature and turbulence quantities are 0.45, 1, 0.6, and 0.6, respectively. However these relaxation factors have been adjusted for each case to accelerate the convergence criterion, which is defined as the relative difference of every dependent variable between iteration steps: Max $\left|\phi^k(i,j) - \phi^{k-1}(i,j)\right| \le 10^{-5}$.

To ensure that the turbulent fluid flow solutions are not significantly affected by the mesh, the numerical simulations are examined under different grid sizes that range from 62×28 to 82×52. Adding grid points beyond 62×28 did not significantly affect the results.

3. Results and discussion

The computations are presented for two-dimensional turbulent flow through a channel with a backward-facing step and impingement cooling. Different contraction ratios and sizes of impinging jets are investigated for different Reynolds numbers.

The velocity vectors for different numbers of impinging jets are shown in Figures(2-4). As Figure (2) shows, the separation and reattachment, and consequently the recirculation regions, are found directly behind the backward-facing step and the impinging jets. The cross flow begins to separate at the edge of the step and forms a recirculation region. The size and strength of this region depends on the expansion ratio and the existing impinging jets. It is evident that the strength of the recirculation region increase. Also the dimensionless re-attachment length((L_T) after the step increase as the contraction ratio (SR) decrease where L_T=2, 2.28, 2.3 as shown in (a), (b) and (c) respectively; this trend is evident in the studied cases. Recirculation between the impinging jets increased as the contraction ratio and number of impinging slot jets increased. It can be seen that the incoming cross flow affects the behaviour of the trajectories of multiple impinging jets because the potential core of each jet is distorted. Part of the flow of impinging jets forms re-circulating regions between the jets, and the other part tries to push the incoming cross flow towards the lower wall of the channel; thus, the combined flow accelerates and becomes narrower. The size of the recirculation region and, consequently, the re-attachment length are affected by the impinging slot jet flow. As the Figure shows, the near upstream impinging jet has a significant effect on this region; it distorts the structure and size of the mentioned recirculation region where the separated flow after the step is pushed towards the bottom wall. As a result, the size and re-attachment length of the recirculation region are minimised. For Figures (3) and (4), the size and strength of the recirculation regions for three and four jets are larger than those with two jets. However, the flow structure is similar for all scenarios. Also, the size and recirculation regions increase as the number of impinging jets increases. The heat transfer is enhanced as the strength of the recirculation regions increases, as shown in Figure (10) where the local Nusselt number increases just after the step between the jets due to the increase in losses.

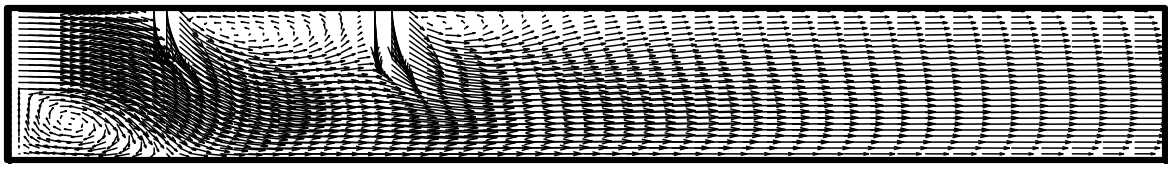

a. SR = 0.5

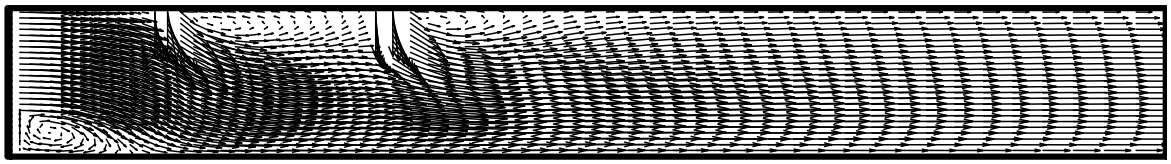

b. SR = 0.35

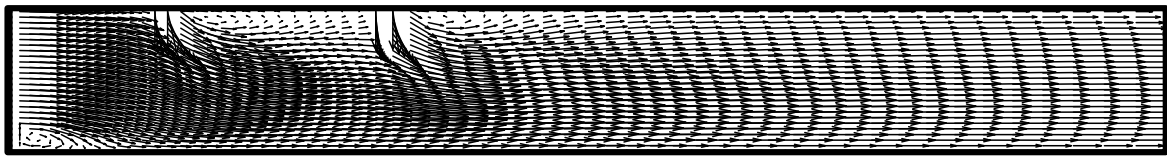

c. SR = 0.25

Figure (2). Computed velocity vectors for 2 jets and different values of step height ratios, Re_j=13517, Re_{in}=16896, H/B=11, and P/B=4.

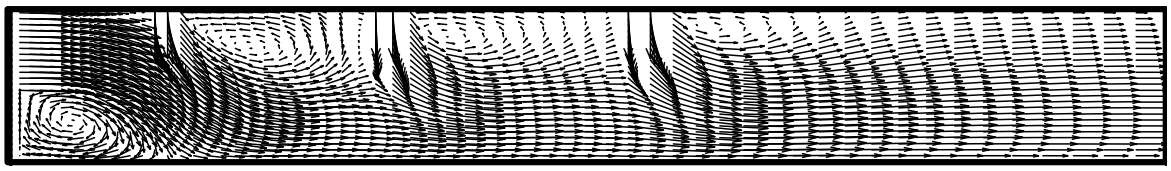

a. SR = 0.5

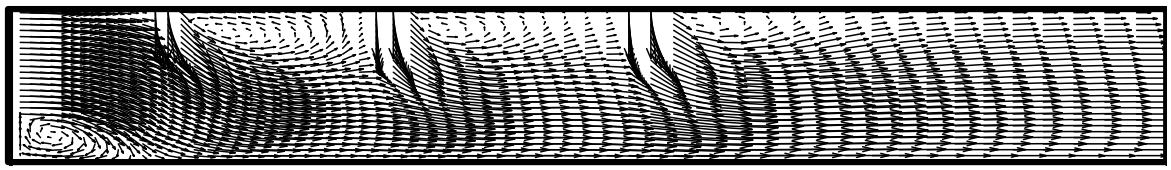

b. SR = 0.35

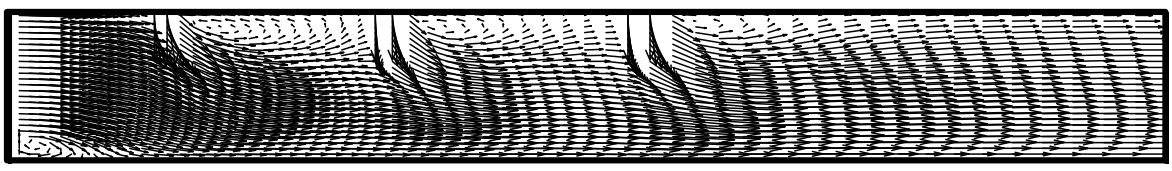

c. SR = 0.25

Figure (3). Computed velocity vectors for 3 jets and different values of step height ratios, Re_j=13517, Re_{in}=16896, H/B=11, and P/B=4.

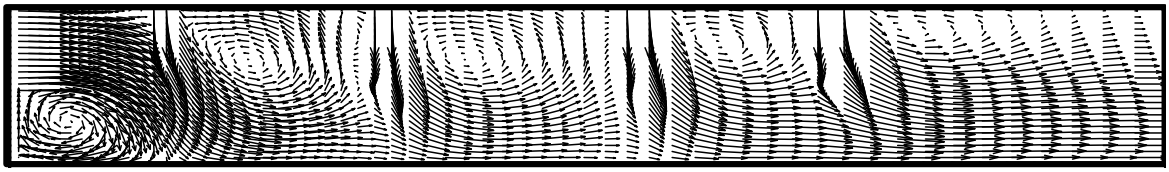

a. SR =0.5

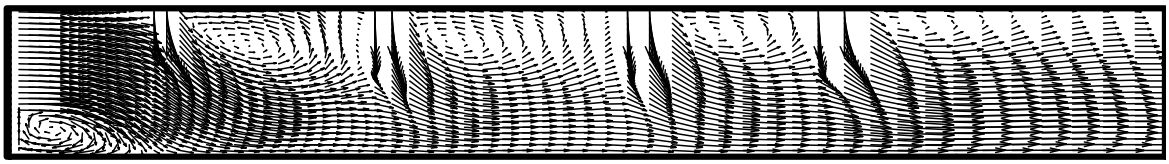

b. SR =0.35

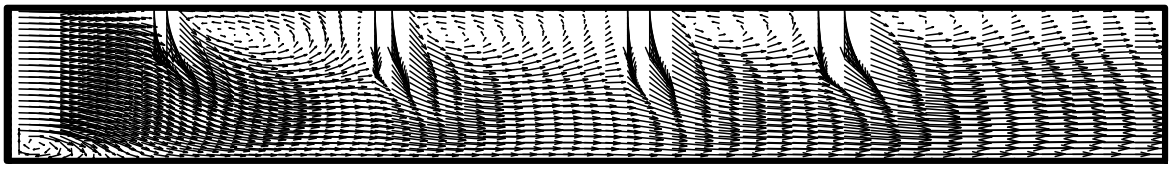

c. SR =0.25

Figure (4). Computed velocity vectors for 4 jets and different values of step height ratios, Re_j=13517, Re_{in}=16896, H/B=11, and P/B=4.

The effect of contraction ratio on the distribution of streamlines for three impinging slot jets and H/B=11 is demonstrated in Figure (5). The trajectories of the impinging slot jet forced the cross channel flow towards the bottom wall of the channel and reduced the reattachment length just after the edge of the step. The flow struck the bottom wall in the region between the step and the first impinging jet and enhanced heat transfer, as shown in Figure (9). This phenomenon occurred for all the studied cases and is enhanced as the contraction ratio increased (the strength of recirculation regions increase). Beyond x=0.1, the rate of heat transfer decreases as the contraction ratio increases. Also, it is clear that the presence of impinging cooling enhances the heat transfer in the considered physical problem, as shown in Figure(10).

Figure (10) illustrates that three jets achieve the optimum rate of heat transfer. When the number of impinging slot jets exceeds three, the rate of heat transfer is significantly decreased beyond x=0.1.

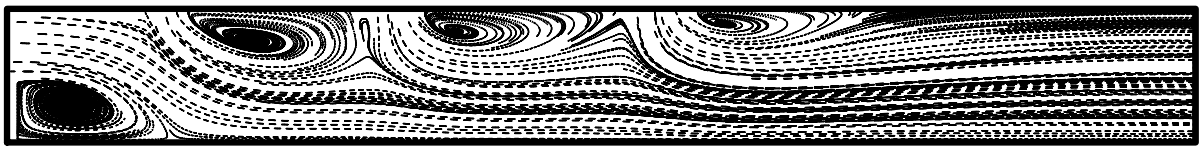

a. SR =0.5

b. SR =0.35

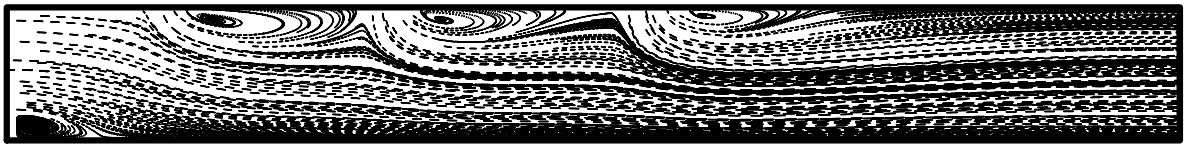

c. SR =0.25

Figure (5). Stream line distribution for 3 jets and different values of step height ratios, Re_j=13517, Re_{in}=16896, H/B=11, and P/B=4.

Figures (6) and (7) demonstrate the effect of increasing the size and number of impinging jets on the computed flow field. The results are presented in the form of velocity vectors and stream lines. It is clear that the strength of recirculation regions behind each jet and the step increase as the slot jet width increases (the ratio H/B decreases). This flow structure is dominant for all the studied cases and affects the heat transfer, as shown in Figure (8). In general, the velocity of the main channel flow near the hot wall increases as the ratio H/B decreases (of the size of the slot jets increases) because the flow passage becomes narrower. The effect of increasing the size of the impinging jets on the distribution of the local Nusselt number is found in Figure (8). It is clear that the local Nusselt number increases as the slot jet width increases (the ratio H/B decreases) because the strength of recirculation regions are

larger behind each jet and the step. The strength recirculation regions increase the impinging flow towards the hot wall and consequently increases the rate of heat transfer.

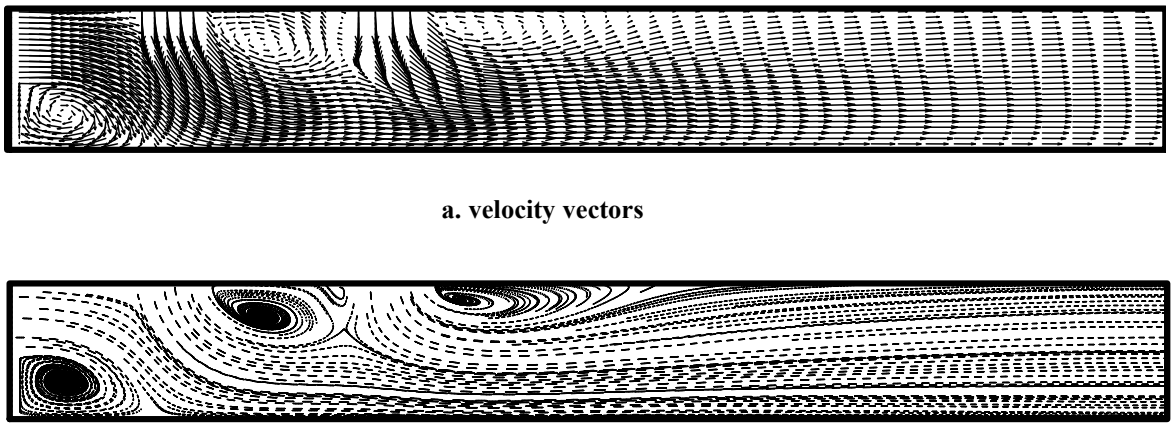

a. velocity vectors

b. stream lines

Figure (6). Effect of slot jet width on the flow field distribution for 2 jets: SR=0.5, Re_j=13517, Re_{in}=16896, H/B=2.5, and P/B=4.

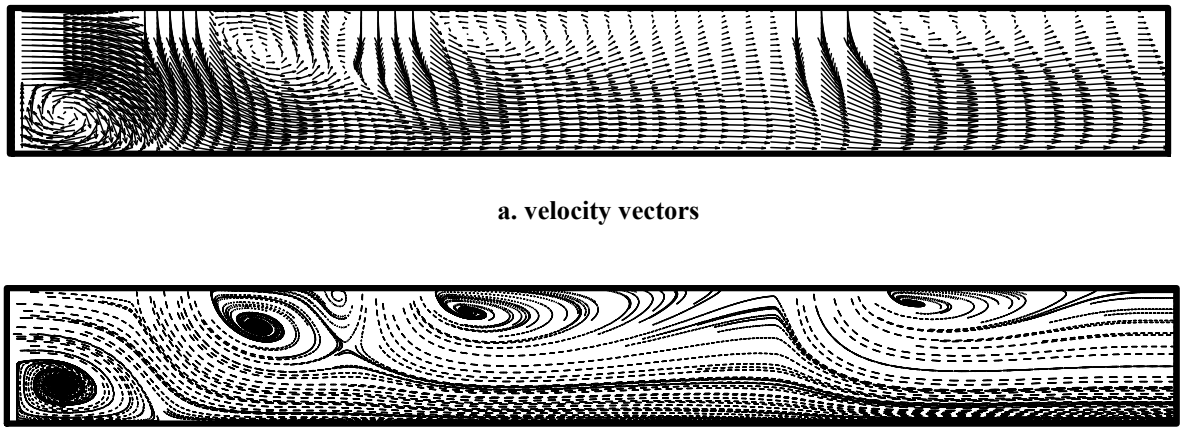

a. velocity vectors

b. stream lines

Figure (7). Effect of a slot jet width on the flow field distribution for 2 jets, SR=0.5, Re_{in}=16896, H/B=2.5, P/B=4

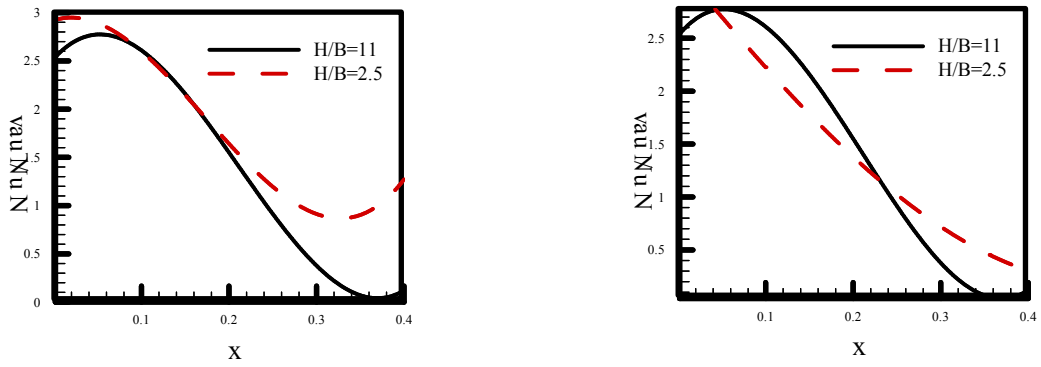

a. 2 jets **b. 3 jets**

Figure (8). Variation of local Nusselt number for SR=0.5, Re_j=13517 and Re_{in}=16896 .

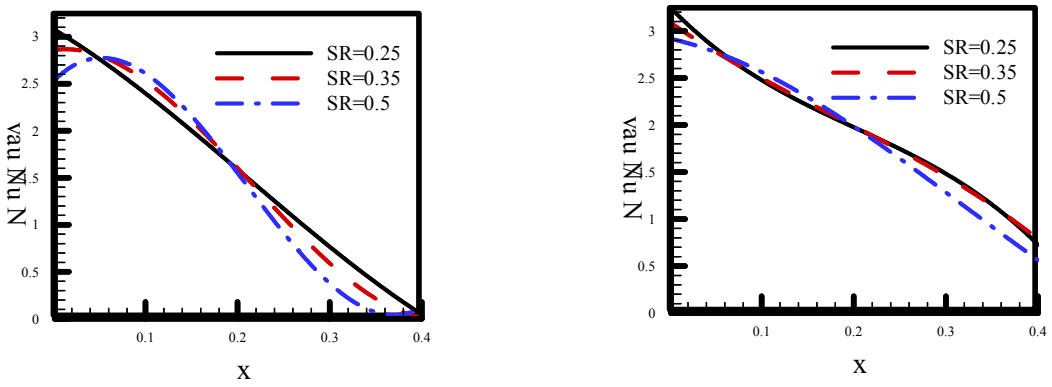

a. 2 jets **b. 3 jets**

Figure (9). Variation of the local Nusselt number with multiple impingement jets, Re_j=13517, Re_{in}=16896, H/B=11, and P/B=4.

Figure (10) represents the variation of local Nusselt number along the hot wall of the backward facing in the presence of impinging jets and without impinging jets. As it is shown, the local Nusselt number is increased significantly in the presence jets compared with that of the case of no jets. Also, it is observed that the three impinging jets indicates the higher rate of heat transfer especially at x> 0.2.

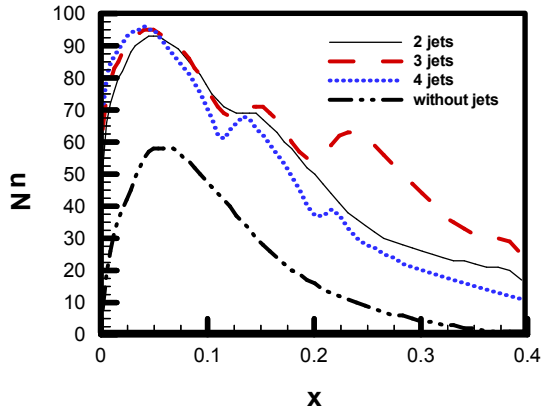

Figure (10). Comparison of variation of local Nusselt number with and without impingement for SR=0.5, Re_j=13517, Re_{in}=16896, H/B=11, P/B=4.

When the impinging jets and inlet channel flow Reynolds numbers increase, the recirculation regions behind each jet increase. However, the recirculation region after the step decreases, as shown in Figure (11). If the Reynolds number increases, the inertia force and penetration of the impinging flow to cross flow increase, which enhances the rate of heat transfer.

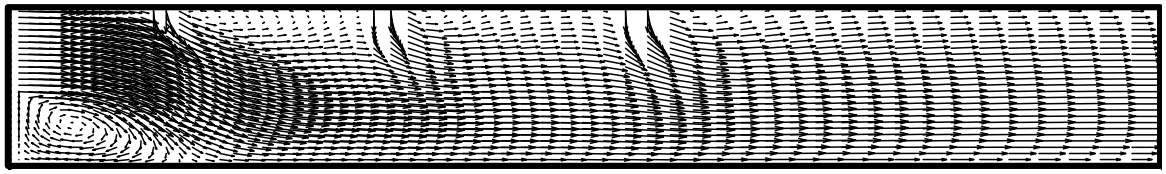

a. Re_j= 6210

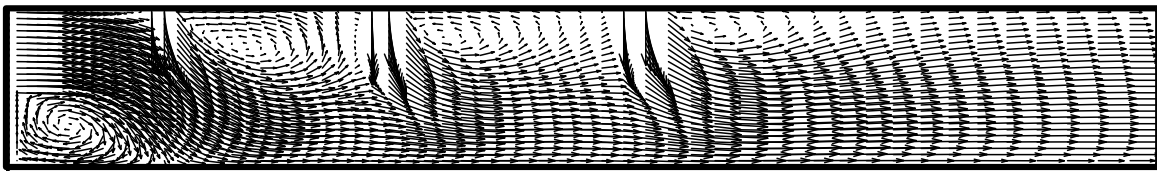

b. Re_j= 13517

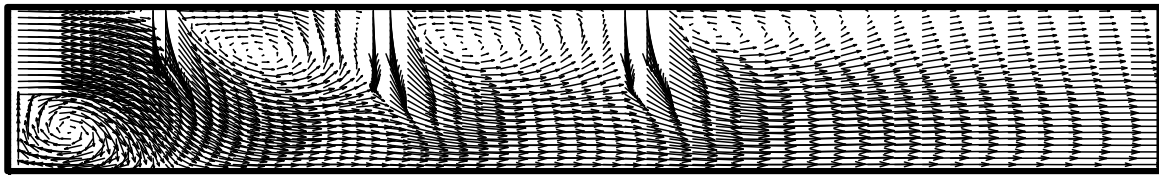

c. Re_j= 28127

Figure (11). Flow field distribution for different jet Reynolds numbers, SR=0.5, H/B=11, P/B=4Re_{in}=16896.

Figure (12) illustrates the non-dimensional axial velocity at different axial positions. For SR=0.5, it is evident that the dimensionless axial velocity increases as Re increases for x/L ≤ 0.1, while the velocity increases and then decreases when x>0.1.

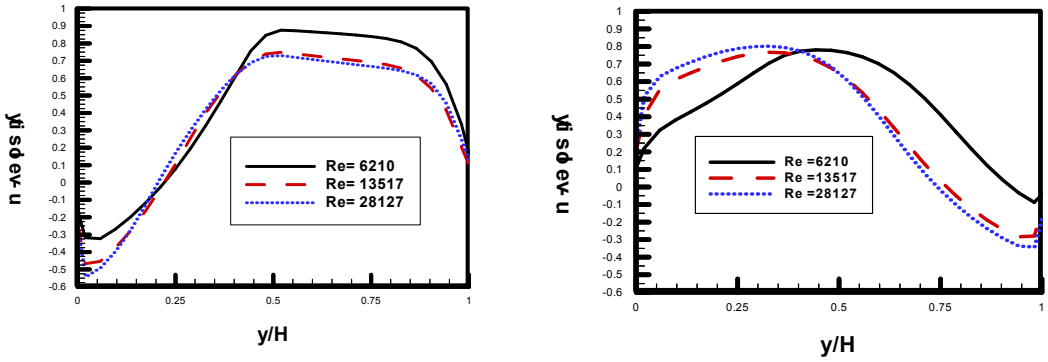

a. x/L=0.0315 **b. x/L=0.2**

Figure (12). Variation of the dimensionless axial velocity (u/U_{in}) at different jet Reynolds numbers: H/B=11, P/B=4, Re_{in}=16896, and SR=0.5 .

The distribution of dimensionless axial velocity is depicted at Figure (13) for 3 impinging sot jets and different contraction ratios. Figure (13) shows that the higher values of the velocity occur at SR=0.25, which confirms that the recirculation regions increase in size as SR increases, as discussed previously.

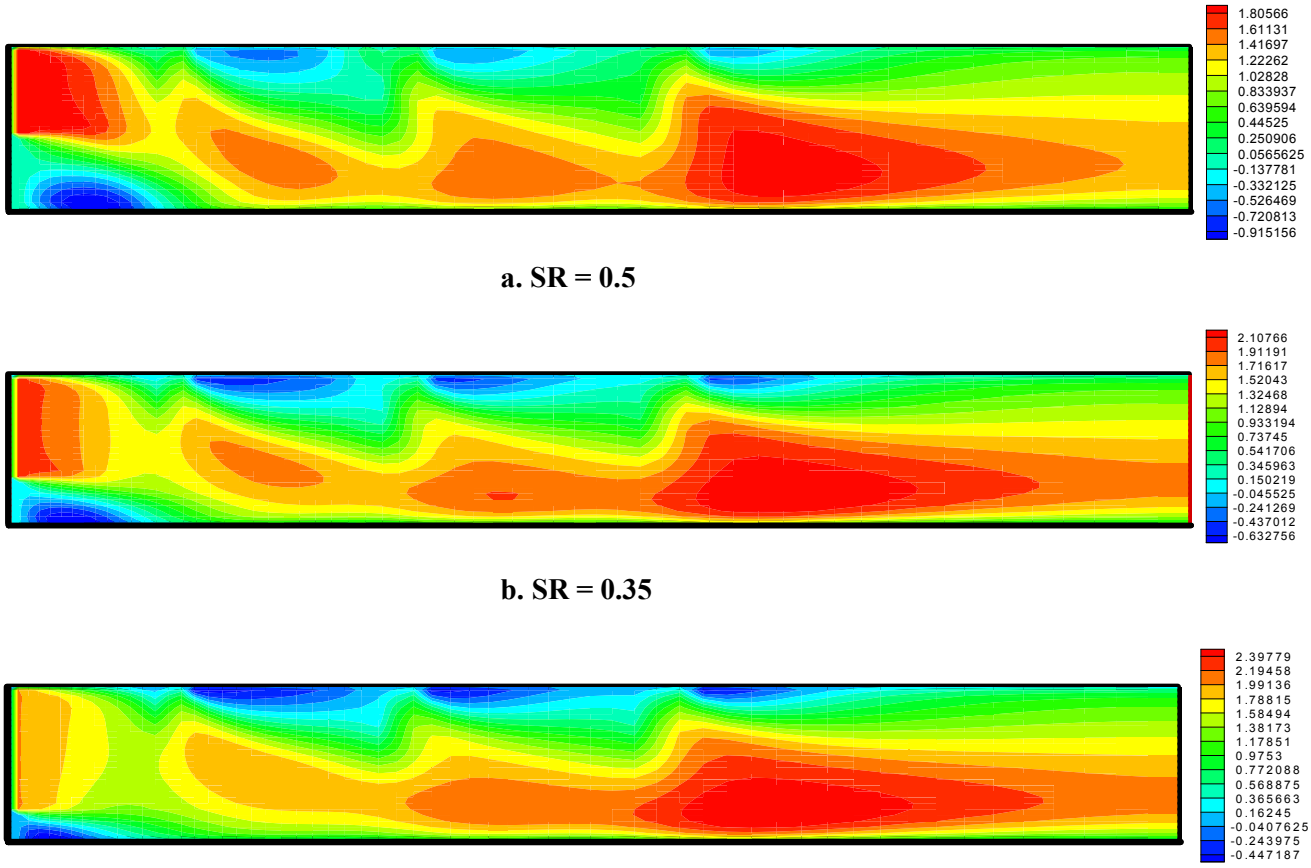

a. SR = 0.5

b. SR = 0.35

c. SR = 0.25

Figure (13). Distribution of dimensionless axial velocity(u/U_{in}) for 3 impingement jets, H/B=11, P/B=4, Re_j=13517, Re_{in}=16896 .

Figure (14) illustrates the variation of the turbulent kinetic energy with different expansion ratios at the upper and lower walls of the channel. When SR=0.5, the turbulent kinetic energy values are higher at the lower wall compared to those at the upper one. This trend extends to the contraction ratio SR=0.25. The maximum and minimum values shown in the curves are due to the effect of the impinging jets .

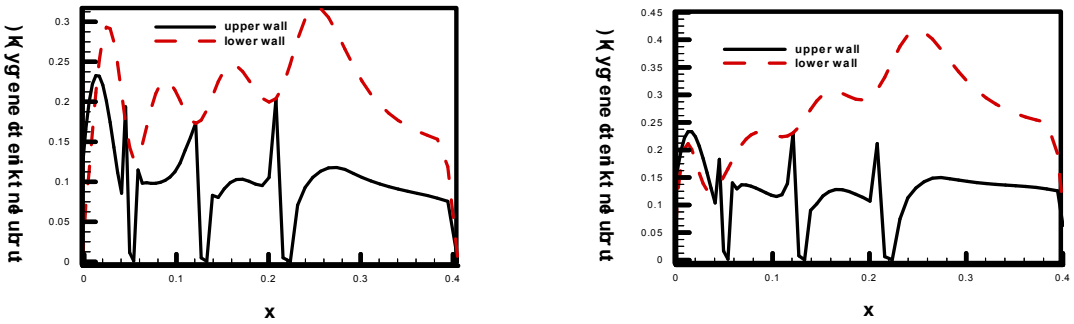

a. SR=0.5 **b. SR=0.25**

Figure (14). Variation of turbulent kinetic energy (at the walls), Re_j=13517, Re_{in}=16896, H/B=11, and P/B=4 .

The effect of Re on the variation of turbulent kinetic energy at y=H/2 is depicted at Figure (15). It can be noted that the turbulent kinetic energy is increased as Re increases. It is expected that the increase of Re increases the stresses and consequently the turbulent kinetic energy increases.

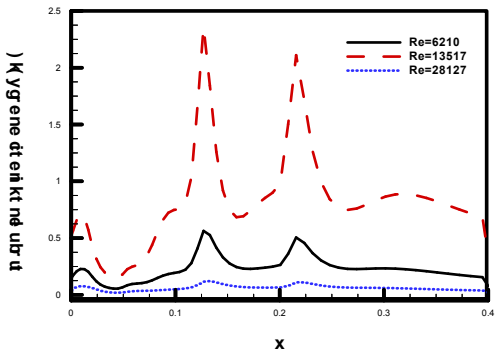

Figure (15). Variation of turbulent kinetic energy for different jet Reynolds numbers (at y = H/2): SR=0.5, Re_{in}=16896, H/B=11, and P/B=4 .

To validate the present numerical code, a test on some of the published studies is performed as shown in Figures (16-18). As the Figures show, acceptable agreement is obtained. However some discrepancy is noticed . This is attributed to use of k-ε model where this model gives un prediction in some of recirculation flows. This un prediction is about 10٪.

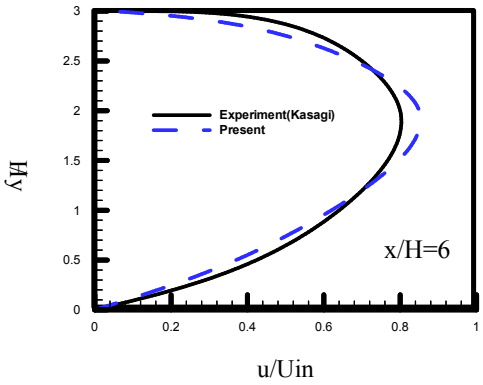

Figure (16). Comparison of the present results with experimental published results of Kasagi(1995), Re=5540.

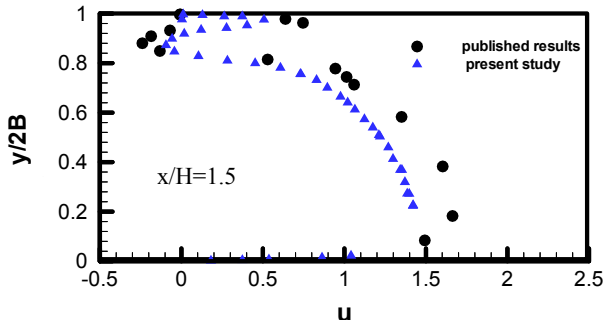

Figure (17) . Comparison between the present results and published experimental data of Lio et al.(1993).

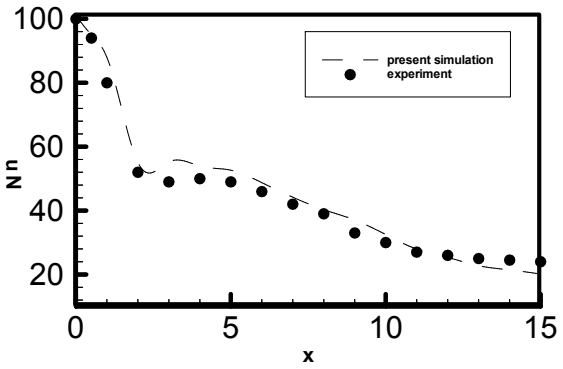

Figure (18). Comparison of the present results with published results of Ichimiya and Hosaka(1992).

4. Conclusions

The following conclusions are obtained from this study.

1. As compared with conventional backward-facing step flow problem, incorporating array of impinging slot jets is significantly enhanced the rate of heat transfer
2. Increasing the number of impinging slot jets enhanced the rate of heat transfer especially near the regions close to the facing step. However this behaviour is converted when number of these jets exceed three.
3. The strength of the recirculation zone behind each slot jet and the step increases as jet width increases.
4. The heat transfer rate increases as the jet size increases.
5. The turbulent kinetic energy is enhanced as the channel and slot jet flow Reynolds numbers increase.

5. References

[1] Lio, T., Hwang, J.,1992, " Developing Heat Transfer and Friction in a Ribbed Rectangular Duct with Flow Separation at Inlet", ASME. J. Heat Transfer, 114, 546-573.

[2] Lio, T.M., Hwang, G.G. , Chen, S.H., 1993, "Simulation and Measurements of Enhanced Turbulent Heat Transfer in Channels With Periodic Ribs on One Principal Wall" International Journal of Heat Mass Transfer, 36,507-507.

[3] Rau, G., Cakan, M., Moeller, D., Arts, T,1988," The Effect of Periodic Ribs on The Local Aerodynamics and Heat Transfer Performance of A Straight Cooling Channel" ASME Journal of Turbomachinery,120, 368-375.

[4] Han, J.C, Heat , 1988, "Transfer and Friction Characteristics in Rectangular Channels With Rib Turbulators" ASME Journal of Heat Transfer,110, 91-98.

[5] Nobuhide Kasagi, Akio Matsunaga,1995," Three- Dimensional particle-Tracking-Velocimeter velocimetry measurement of Turbulennce Statistics and Energy Budget in a backward-Facing Step Flow" Int. J. Heat and Fluid Flow,16, 477-485.

[6] Srba Jovice, David M. Driver, 1994 ," Backward Facing Step Measurements at Low Reynolds Number, R_{eh}=500", NASA, California 94035-1000.

[7] Abe, K., Kondoh, T., 1994, "A new Turbulent Model for Predicting Fluid Flow and Heat transfer in Separating and Reattacing flows", 37,139-151.

[8] Ichimiya, K., Hosaka, N., 1992 ,"Experimental Study of Heat Transfer Characteristics Due To Confined Impinging Two Dimensional Jet" Exp. Thermal and Fluid Science, 5,803-807.

[9] Zhang, H.Q., Chan, C. K., Lau, K.S, 2001 ," Numerical Solution of Sudden Expansion Particle-Laden Flows Using an Improved Stochastic Flow Model", Numerical Heat Transfer, Part A, 4089-102.

[10] Wang, B., Zhang, H.Q., Wang, X.L., 2006, " Large Eddy Simulation of Particle Response to Turbulence Along Its Trajectory in a Back Word-Facing Step Turbulent Flow", Int. J. Heat Mass Transfer, 49, 415-420.

[11] Thangam, S., Knight, D., 1989, " Effect of Step Height on The Separated Flow Past a Backward Facing Step", Phys. Fluids, 3, 604-606.

[12] Nie, J.H., Armaly, B.F., 2002, " Three Dimensional Convective Flow Adjacent to a Backward Facing Step-effects of Step Height", Int. J. Heat Mass Transfer, 45, 2431-2438.

[13] Rhee, G. H., Sung, H.G., 2000, " Enhancement of Heat Transfer in Turbulent Separated and Re-Attachment Flow by Local Forcing", Numerical Heat Transfer, Part A, l37, 733-735.

[14] KE Feng, Liu Ying-Zheng , Chen Han-Ping, 2007,'' Simultaneous Flow Visualization and Wall Pressure Measurement of the Turbulent Separated and Re-attachment Flow Over a Backward Facing Step", J. Hydrodynamics, 119, 108-187.

[15] Law, H.S., Masliyah, J.H**.,** 1984 **,"**Mass Transfer Due to Confined Laminar Impinging Two Dimensional Jet", Int. J. Heat Mass Transfer, 27, 529-539.

[16] Chou, Y.J., Hung, Y.H., 1994 ,"Impinging Cooling of an Isothermally Heated Surface", ASME. J. Heat Transfer, 116, 479-482.

[17] Lee, X.C., Xheng, Q., Zhung, Y., Tia, Y.Q., 1997," Numerical Study of Recovery Effect and Impingement Heat Transfer with Submerged Circular Jets of Large Prandtl Number Liquid", Int. J. Heat Mass Transfer, 40, 2647-2653.

[18] Behnia, M., Parneix, S., Shabany, Y., Durby, P.A., 1999,"Numerical Study of Turbulent Heat Transfer in Confined and Unconfined Impinging Jets", Int. J. Heat Fluid Flow, 20, 1-9.

[19] Cooper, D., Jackson, C., Launder, B.E., Liao, G.X., 1993, "Impingement Jet Studies for Turbulence Model Assessment-I Flow Field Experiments", Int. J. Heat Mass Transfer, 36, 2675-2684.

[20] Park, T.S., Sung, H.j., 2001," Development of Near Wall Turbulence Model and Application to Jet Impingement Heat Transfer, Int J. Heat Fluid Flow, 22, 10-18.

[21] Beitmal, A.H., Saad, M.A., Patel, C.D., 2000, "Effects of Surface Roughness on The Average Heat Transfer of An Impinging Air Jet", International Communications in Heat and Mass Transfer, 27, 1-12.

[22] Yang, Y.T., Shyu, C.H., 1999," Numerical Study of Multiple Impinging Slot Jets With an Inclined Confinement Surface", Numerical Heat Transfer, Part A, 33, 23-37.

[23] EL-Gabry, Lamyaa, A., Kamiski, Deborah, A., 2005, "Numerical Investigation of Jet Impingement with Cross Flow-Comparison of Yang-Shih And Standard k-ϵ Turbulence Models", Numerical Heat Transfer, Part A, 47, 441-469.

[24] Craft, T.G., Graham, L.G.W., Launder, B.E., 1993,"Impinging Jet Studies For Turbulence Model Assessment-II-An Examination of the Performance of Four Turbulence Models", Int. J. Heat Mass Transfer, 36, 2685-2697.

[25] Shou Shing Hsieh, Jung-Tai Huang, Huang-Hsiu Tsai, 2003, "Impingement Cooling in a Rotating Square Annular Duct with Cross Flow Effect From Rib-Roughened Surface", Int. J. Heat Mass Transfer, 39.

[26] Jones, W.P., Lunder, B.E., 1972,"The Prediction of Laminarization with a Two Equation Model of Turbulence", J. Heat Mass transfer.

[27] Versteege, H.K., Malalasekera, W., 1995, "An Introduction of Computational Fluid Dynamics", Hemisophere Publishing Corporation, United State of America.

6. Nomenclature

G	generation term, $Kg/m.sec^3$
H	height of the channel, m
k	turbulent kinetic energy, m^2/s^2
L	length of the channel, m
L_T	reattachment length behind the facing step(X_{cr}/s)
Nu	local Nusselt number, -
Nuav	average Nusselt number
p	pitch, m
P	pressure, N/m^2
Pr	Prandtl number, -

Re	Reynolds number,-
s	step height, m
SR	contraction ratio (s/H),-
T_C	cold wall temperature, Ċ
T_H	hot wall temperature, Ċ
$\overline{\rho u_i u_j}$	Reynolds stresses
$\overline{\rho u_i t_j}$	turbulent heat fluxes
U_{in}	velocity at a channel inlet
U_j	velocity at a slot jet inlet
X_{cr}	the reattacing distance behind the step

Greek symbols:

ϵ	turbulence dissipation rate, m^2/s^3
μ	dynamic viscosity, $N.s/m^2$
μ_t	turbulent viscosity, $N.s/m^2$
ρ	air density, Kg/m^3
Γ_{eff}	effective exchange coefficient, kg/m.s
θ	dimensionless temperature $\left(\frac{T-T_c}{T_h-T_c}\right)$, -
σ_k; σ_ϵ	turbulent Schmidt numbers, -
α	thermal diffusivity of fluid, m^2/s
S_ϕ	source term, -
ϕ	constant property, -